

# Modeling, Analysis and Control of Hexagram Inverter for Three-Phase Induction Motor Drive

K.Rajambal

Department of Electrical and Electronics Engineering  
Pondicherry Engineering College, Pondicherry, India  
E-mail: rajambalk@gmail.com

G.Renukadevi

Department of Electrical and Electronics Engineering  
Pondicherry Engineering College, Pondicherry, India  
E-mail: renunila\_1977@yahoo.com

## Abstract

This paper presents the modeling, analysis and control of Hexagram inverter for three phase induction motor drive configuration. The Hexagram inverter can be used for both three phase and six phase applications. It has many advantages including reduced number of switches, modular structure leading to easy construction and maintenance, isolated dc buses. Besides, it has built-in fault redundancy due to the module interconnection. It has lowered dc energy storage requirement compared to that of cascaded H-bridge inverter. This eminent feature makes the system in high power applications. A simulation model of the Hexagram inverter fed three phase induction motor drive is developed in Matlab/Simulink environment. Simulation is carried out to study the drive performance at different operating conditions and the results are presented.

**Keywords:** closed loop control, fault tolerant feature, hexagram inverter, three phase induction motor drive

## 1. Introduction

The medium-voltage (MV) converters have become a new breed in high-power applications. Numerous MV topologies have been proposed and investigated since the mid 1980s (Jose Rodriguez 2002 - Krug 2004). The development and application of MV variable speed drives (VSDs) have brought significant advantages in improved process control, higher efficiency, and energy savings to the industry (Cheng 2006). From the survey articles (Carrasco 2006 - Kim 2004) it becomes clear that three topologies are favored by MV drive manufacturers: Neutral-point-clamped (NPC) inverter (Bendre 2006-Vargas 2007); Flying capacitor (FC) inverter (Kim 2004); and cascaded H-bridge (CHB) inverter (Du 2006 - Rech 2007). A high-voltage fast recovery diode is used to clamp the voltage in NPC configuration. The configuration suffers from voltage unbalancing, neutral point stabilization at heavy or dynamic loading, higher THD and the requirement of LC filter to reduce the vibration and noise of the machine. The FC configuration is used to clamp the voltage and overcome some of the drawbacks of NPC configuration. However the number of capacitors required increases, when the number of levels is high and complex precharge circuits are needed (Kim 2004). At present, the cascaded H-bridge inverter is the best-selling product in the MV ASD market worldwide (Robicon). With the modular structure, the cascaded H-bridge inverter is easy to construction and maintenance. And with the separate dc buses, there is no voltage unbalancing problem. However, despite its many advantages, the cascaded H-bridge inverter still suffers from following drawbacks (Cengelci 1999). It employs a large number of single-phase inverter modules, isolated secondary windings in the input transformer, and three-phase diode rectifiers, resulting in high manufacturing cost. The dc-bus capacitive energy storage requirement is high due to the single-phase structure. It does not have built-in fault tolerant feature so that additional inverter modules are necessary to provide redundancy. The problems can be overcome by a new multilevel inverter – Hexagram inverter (Wen & Smedley). The structure of the Hexagram inverter is shown in Figure 1 (a). The new topology is composed of six interconnected VSIs in the form of six switch module as shown in the circle in Figure 1 (b). The connection between the modules is depicted with a connection diagram.

There are six inner inductors connecting any of the two modules in order to limit the circulating current. With synchronized control signals, small value inductors will be sufficient to limit the circulating current to a low

value. Figure 1(c) shows the connection diagram, in which each triangle specifies the each inverter bridge and the inner legs any two of the VSI modules interconnected to the inductors, and the outer legs are connected with motor terminals. Differing to the three-phase VSI, the Hexagram inverter has six output terminals, which provides two options to either drive a three-phase motor (neutral not connected) or drive a six-phase motor. This paper will focus on the Hexagram inverter applied for a three-phase motor drive (Wen & Smedley 2008) and the star connected six phase drive (Wen & Smedley 2007). The new Hexagram inverter has a modular structure and no voltage balancing concern as the cascaded H-bridge inverter; in addition, it has following superior characteristics:

- Fewer diode bridge rectifiers, inverter modules, and input transformer secondary windings are required to achieve the power level.
- Lower dc-link capacitive energy storage requirement due to the three-phase structure. In balanced systems, the instantaneous power of each six-switch module is constant so that the capacitors are not subject to low-frequency power ripples.
- Due to the interconnected structure, Hexagram inverter has built-in redundancy for fault tolerance. The inner legs of the Hexagram inverter which are not directly connected to the load are connected in a closed-loop. Therefore, if some switch of the inner leg fails (open), the overall inverter is capable of operating at a reduced power level.
- The voltage stress of this inverter is reduced three times compared to a two-level inverter with the same output voltage.

In addition, well developed Indirect field oriented control schemes and well developed SPWM techniques for VSI can be directly applied, and the six modules inside Hexagram inverter equally share the output power so that the components of the inverter no need to be over designed. With the symmetrical and naturally balanced structure, the proposed Hexagram inverter has many inherent advantages. Detailed analysis of the inverter will be conducted in section 2 to section 6, after that simulation and experiment results will be given to verify the analysis in section 7 and 8, then a brief conclusion will be provided in section 9.

## 2. Hexagram Inverter for a Three Phase Induction Motor Drive

Figure 2 shows a complete MV ASD system, composed of a transformer with six secondary windings, six diode rectifiers, six dc capacitors and a Hexagram inverter (Wen & Smedley 2008). The transformer shown is an 18-pulse transformer, with six Secondary windings arranged in  $0^\circ, \pm 20^\circ$  phase shift (two are identical), to achieve harmonic current cancellation in the utility line currents, leading to clean input power. The input current total harmonic distortion (THD) for 18-pulse rectifier is about 5-6%. The six secondary windings can also be arranged in  $\pm 5^\circ, \pm 15^\circ, \pm 25^\circ$  phase shift to form a 36-pulse rectifier to further reduce the input current harmonics, if necessary. Diode rectifiers and dc capacitors are used to convert the three-phase ac to dc to provide the isolated dc buses for the Hexagram inverter. Replacing the diode rectifiers with the pulse width modulation (PWM) voltage source converters will enable the VSD system with the capability of regenerative braking (Wen & Smedley 2008).

## 3. Analysis of Hexagram Inverter

### 3.1 Voltage Relationship

The phasor diagram of the VSI module of Hexagram inverter is shown in Figure 3. Phase Voltages of VSI modules are shown in Figure 3 (a). It is seen that the phase of the VSI module is  $V$  volts whereas the output voltage is  $3V$  for Hexagram inverter as shown in Figure 3 (b). The rms phase voltages of the VSI modules are given in equation(1).

$$\begin{bmatrix} V_{a1\omega} \\ V_{b1\omega} \\ V_{c1\omega} \end{bmatrix} = \begin{bmatrix} V_{a3\omega} \\ V_{b3\omega} \\ V_{c3\omega} \end{bmatrix} = \begin{bmatrix} V_{a5\omega} \\ V_{b5\omega} \\ V_{c5\omega} \end{bmatrix} = \begin{bmatrix} V_{a2\omega} \\ V_{b2\omega} \\ V_{c2\omega} \end{bmatrix} = \begin{bmatrix} V_{a4\omega} \\ V_{b4\omega} \\ V_{c4\omega} \end{bmatrix} = \begin{bmatrix} V_{a6\omega} \\ V_{b6\omega} \\ V_{c6\omega} \end{bmatrix} \quad (1)$$

Where  $\omega$  is the frequency of the voltage in radius. (It should be noted that (1) is true with restrictions on the modulation strategy. For example, for sinusoidal pulse width modulation (SPWM), the switching frequency should be an integer multiple of six times the fundamental frequency). Then, the fundamental output voltages of

the Hexagram inverter are determined and given in the equation (2).

$$\begin{bmatrix} v_{AO} \\ v_{BO} \\ v_{CO} \end{bmatrix} = - \begin{bmatrix} v_{A'O} \\ v_{B'O} \\ v_{C'O} \end{bmatrix} = \begin{bmatrix} 3\sqrt{2}V \sin(\omega t) \\ 3\sqrt{2}V \sin(\omega t - 120^\circ) \\ 3\sqrt{2}V \sin(\omega t + 120^\circ) \end{bmatrix} \quad (2)$$

From the equation (2) the output voltage of Hexagram inverter are three times of the VSI modules.

### 3.2 Current Relationship

Assume that the Hexagram inverter is connected to a symmetrical three-phase load. According to (2), the three-phase output currents can be expressed as

$$\begin{bmatrix} i_A \\ i_B \\ i_C \end{bmatrix} = \begin{bmatrix} i_{a1} \\ i_{b3} \\ i_{c5} \end{bmatrix} = - \begin{bmatrix} i_{A'} \\ i_{B'} \\ i_{C'} \end{bmatrix} = - \begin{bmatrix} i_{a4} \\ i_{b6} \\ i_{c2} \end{bmatrix} = \begin{bmatrix} \sqrt{2}I \sin(\omega t) \\ \sqrt{2}I \sin(\omega t - 120^\circ) \\ \sqrt{2}I \sin(\omega t + 120^\circ) \end{bmatrix} \quad (3)$$

The phase currents of the six VSI modules satisfy the following equation:

$$\begin{bmatrix} i_{a1} + i_{b1} + i_{c1} \\ i_{a2} + i_{b2} + i_{c2} \\ i_{a3} + i_{b3} + i_{c3} \\ i_{a4} + i_{b4} + i_{c4} \\ i_{a5} + i_{b5} + i_{c5} \\ i_{a6} + i_{b6} + i_{c6} \end{bmatrix} = 0 \quad (4)$$

Any two of the six modules are interconnected so that the currents inside the inverter have the following relationship:

$$\begin{bmatrix} i_{b1} \\ i_{a2} \\ i_{c3} \\ i_{b4} \\ i_{a5} \\ i_{c6} \end{bmatrix} = - \begin{bmatrix} i_{b2} \\ i_{a3} \\ i_{c4} \\ i_{b5} \\ i_{a6} \\ i_{c1} \end{bmatrix} \quad (5)$$

With the inductors, the circulating current in the loop formed by the connection of the six modules is limited to a low value and can be neglected as

$$i_{b1} + i_{a2} + i_{c3} + i_{b4} + i_{a5} + i_{c6} = 0 \quad (6)$$

Combining (3)–(6), gives the result that module 1, 3, 5 have the same phase currents as  $i_A$ ,  $i_B$ ,  $i_C$ , and module 2, 4, 6 have the same phase currents as  $-i_A$ ,  $-i_B$ ,  $-i_C$ . The result is expressed in equation (7) and (8).

$$\begin{bmatrix} i_{a1} \\ i_{b1} \\ i_{c1} \end{bmatrix} = \begin{bmatrix} i_{a3} \\ i_{b3} \\ i_{c3} \end{bmatrix} = \begin{bmatrix} i_{a5} \\ i_{b5} \\ i_{c5} \end{bmatrix} = \begin{bmatrix} \sqrt{2}I \sin(\omega t) \\ \sqrt{2}I \sin(\omega t - 120^\circ) \\ \sqrt{2}I \sin(\omega t + 120^\circ) \end{bmatrix} \quad (7)$$

$$\begin{bmatrix} i_{a2} \\ i_{b2} \\ i_{c2} \end{bmatrix} = \begin{bmatrix} i_{a4} \\ i_{b4} \\ i_{c4} \end{bmatrix} = \begin{bmatrix} i_{a6} \\ i_{b6} \\ i_{c6} \end{bmatrix} = \begin{bmatrix} \sqrt{2}I \sin(\omega t - 180^\circ) \\ \sqrt{2}I \sin(\omega t + 60^\circ) \\ \sqrt{2}I \sin(\omega t - 60^\circ) \end{bmatrix} \quad (8)$$

This result indicates that when the Hexagram inverter is connected to a symmetrical load, the phase currents of all six modules are identical. The current phasor diagram is depicted in Figure 4. Where the currents lagging the corresponding voltages by  $\theta$  degree. The phase angle  $\theta$  is dependent on the load characteristics. The instantaneous power of the six modules is derived from (2) and (8) as

$$p_I(t) = p_{II}(t) = p_{III}(t) = p_{IV}(t) = p_V(t) = p_{VI}(t) = 3VI \cos \theta \quad (9)$$

This result indicates that the six modules have equal output power, and the instantaneous power through each module is constant, so that the dc energy storage requirement is low and the dc capacitor can be sized small.

#### 4. Equivalent Circuit of the Hexagram Inverter

The equivalent circuit of the circulating current loop is depicted in Figure 5. where  $L_{12}, L_{23}, L_{34}, L_{45}, L_{56}$  and  $L_{61}$  are the inductances of the inductors between any two of the six modules;  $V_{b1c1}, V_{a2b2}, V_{c3a3}, V_{b4c4}, V_{a5b5}$  and  $V_{c6a6}$  are the instantaneous voltages depending upon the switching of the inverter, and  $i_{L12}, i_{L23}, i_{L34}, i_{L45}, i_{L56}$  and  $i_{L61}$  are the inductor currents derived under the zero circulating current condition and satisfy the following equation:

$$\begin{bmatrix} i_{L12} \\ i_{L23} \\ i_{L34} \\ i_{L45} \\ i_{L56} \\ i_{L61} \end{bmatrix} = \begin{bmatrix} i_{b1} \\ i_{a2} \\ i_{c3} \\ i_{b4} \\ i_{a5} \\ i_{c6} \end{bmatrix} = \begin{bmatrix} i_{b3} \\ i_{a4} \\ i_{c5} \\ i_{b6} \\ i_{a1} \\ i_{c2} \end{bmatrix} \quad (10)$$

The loop voltage defined as the summation of the equivalent voltage sources in the circulating current loop is calculated as given in equation (11)

$$v_{loop} = v_{b1c2} + v_{a2b2} + v_{c3a3} + v_{b4c4} + v_{a5b5} + v_{c6a6} + L_{12} \frac{di_{L12}}{dt} + L_{23} \frac{di_{L23}}{dt} + L_{34} \frac{di_{L34}}{dt} + L_{45} \frac{di_{L45}}{dt} + L_{56} \frac{di_{L56}}{dt} + L_{61} \frac{di_{L61}}{dt} \quad (11)$$

The circulating current will occur when the loop voltage is not zero. Moreover, the inductor currents can be viewed as the summation of the currents derived at the zero circulating current condition as given in equation (10) and the circulating current is

$$\begin{bmatrix} i'_{L12} \\ i'_{L23} \\ i'_{L34} \\ i'_{L45} \\ i'_{L56} \\ i'_{L61} \end{bmatrix} = \begin{bmatrix} i_{L12} \\ i_{L23} \\ i_{L34} \\ i_{L45} \\ i_{L56} \\ i_{L61} \end{bmatrix} + i_{loop} \quad (12)$$

In equation (11),  $(V_{b1c1} + V_{a2b2} + V_{c3a3} + V_{b4c4} + V_{a5b5} + V_{c6a6})$  is the major part, since the rest of the part equals 0 at the equal inductance condition according to (9) and (11); even if not, it is small due to the small inductances. In the ideal situations  $(V_{b1c1} + V_{a2b2} + V_{c3a3} + V_{b4c4} + V_{a5b5} + V_{c6a6})$  equals 0 as well. However, both unmatched switching and unequal dc buses will cause it to be nonzero and result in the occurrence of the circulating current. The unmatched switching has very short time duration; small inductances such as several micro henrys are sufficient to limit the circulating current. Consequently, the unequal dc bus is the major cause of the circulating current. By having the first and fourth secondary windings of the transformer of the same phase angle, so are the third and sixth, and fifth and second; the unequal dc bus condition caused by the ripple voltages of the rectification will be entirely eliminated.

#### 5. Closed Loop Control of Hexagram Inverter

The vector control of ac drives has been widely used in high performance control system. Indirect field oriented control (IFOC) is one of the most effective vector control of induction motor due to the simplicity of designing and construction. In order to obtain the high performance of torque and speed of an IM drive, the rotor flux and

torque generating current components of stator current must be decoupled suitably respective to the rotor flux vector like separately excited dc motor. Figure 6 shows the complete schematic of indirect field oriented control for induction motor drive. The torque command is generated as a function of the speed error signal, generally processed through a PI controller. The torque and flux command are processed in the calculation block. The three phase reference current generated from the functional block is compared with the actual current in the hysteresis band current controller and the controller takes the necessary action to produce PWM pulses. The PWM pulses are used to trigger the voltage source inverter to drive the Induction motor. The Performance of the indirect vector controlled drive has been analyzed for varying speed and torque. A PI controller is designed to adjust the modulation index of the Hexagram inverter. From the simulation results it is found that the controller tracks the reference speed is better at high speed range. In the low speed range the speed error increases considerably and the PI controller needs further tuning to achieve better performance. This can be done using Artificial intelligence techniques.

## 6. Comparison of Hexagram Inverter with CHB Inverter

A comparison of the Hexagram inverter and the CHB inverter is given in Table 1 due to their similarity in modular structure and isolated dc buses. From Table 1, following conclusions are obtained:

- Cascaded H-bridge inverter requires more components than Hexagram inverter: six more transformer secondary isolated windings; six more diode rectifiers, twelve more semiconductor switches, six more capacitors. Although Hexagram inverter needs six inner inductors to block the circulating current, the inductors are very small with all modules synchronize controlled.
- The capacitive energy storage requirement is low in the Hexagram inverter, since the instantaneous power through each power module is constant, while the cascaded H-bridge inverter has low-frequency pulsating power caused by the single-phase nature.
- With fewer components and lower component requirement, Hexagram inverter has less manufacturing cost and higher reliability, which makes it a competitive topology for medium voltage variable speed drive applications.

## 7. Simulation Results

The three phase induction motor drive with Hexagram inverter is simulated in Matlab/Simulink environment with the parameters given in Appendix. The switching frequency for SPWM pulses is 1KHz, and the inner inductors are 50 $\mu$ H each. Figure 7 shows simulation results at rated condition for a modulation index of 0.8. Figure 7 (a) shows the 18 pulse transformer output with a phase shift of 0°,  $\pm 20^\circ$  at the three secondaries. The other three secondaries will have the same phase shifts to achieve harmonic current cancellation in the utility line currents, leading to clean input power. Figure 7 (b) shows the rectifier output and the voltage and current of Hexagram inverter respectively. The steady state results showing the output voltage of the inverter and speed of the induction motor for different modulation indices is shown in Table 2. A closed loop response of Hexagram inverter with indirect field oriented control is analyzed for different operating conditions and the results are presented in Figure 8. The speed reference is set at different values and the actual speed, torque, voltage and stator current are observed and presented in Figure 8. The load torque is set at different values and the speed, torque, voltage and stator current variations are shown in Figure 9. It is seen that the indirect field oriented controller tracks the reference speed is less than 1 sec without exceeding the design limits. The performance of the drive under low speed/less load operating conditions are studied through simulation and presented in Figure 10. The closed loop control of Hexagram drive has better performance in the low range of speed and torque conditions.

## 8. Fault tolerant feature of the Hexagram inverter

The  $a_2$  to  $a_3$  leg of the inverter is opened and the output voltages and the current waveforms of the Hexagram inverter are observed. It is seen from Figure (11) that the inverter output is reduced to 290.69V and 12.65 amps respectively at rated condition when the inner leg  $a_2$  to  $a_3$  opened. Therefore, the overall inverter is capable of operating at a reduced power level.

## 9. Conclusion

The performance investigation of Hexagram inverter for a three phase induction motor drive is carried out for medium voltage high power applications. The simulation model of the Hexagram inverter is developed in Matlab/Simulink environment. The performance of the Hexagram inverter is analyzed into SPWM technique. The Hexagram inverter has reduced component count and requirement, built-in fault tolerance, and full utilization of the three-phase structure, which makes it a superior topology for high power applications. A closed loop indirect field oriented controller is designed and its performance is studied for different speed and torque conditions. It is seen that the controller tracks the reference speed is better at high speed range. In the low speed range the speed error increases considerably and the PI controller needs further tuning to achieve better performance. This can be done using artificial intelligence techniques.

APPENDIX

Parameters of the three phase induction motor

PARAMETERS	VALUES
Power	7.5KW(10hp)
Voltage	400V
Frequency	50 Hz
No. of poles	4
Stator resistance (Rs)	0.7384 ohm
Rotor resistance (Rr)	0.7402 ohm
Stator inductance (Ls)	0.003045 H
Rotor inductance (Lr)	0.003045 H
Mutual inductance (Lm)	0.1241 H
Inertia (J)	0.0343 kg.m <sup>2</sup>
Friction (F)	0.000503 N.m.s

References

Jose Rodriguez, Jih-Sheng Lai & Fangzheng Peng (2002), "Multilevel inverters: a survey of topologies, controls, and applications," IEEE Transactions on Industrial Electronics, vol. 49, No. 4.

Chong. K.H. J & Klug R. D. (2004), "High power medium voltage drives," in Proc. Power Con, Singapore, Nov. 21–24, pp. 658–664.

Bernet.S. (2000), "Recent developments of high power converters for industry and traction applications," IEEE Trans. Power Electron., vol. 15, no. 6, pp. 1102– 1117.

Krug.D, Malinowski.M & Bernet.S. (2004), "Design and comparison of medium voltage multi-level converters for industry applications," in Conf. Rec. IEEE IAS Annu. Meeting, vol. 2, pp. 781–790.

Cheng.Y, Qian.C, Crow M. L, Pekarek.S & Atcitty.S. (2006), "A comparison of diode- clamped and cascaded multilevel converters for a STATCOM with energy storage," IEEE Trans. Ind. Electron., vol. 53, no. 5, pp. 1512– 1521.

Carrasco. J. M, Franquelo. L. G, Bialasiewicz .J.T, Galvan.E, PortilloGuisado. R. C, Prats., M. A. M, Leon. J. I & Moreno-Alfonso.N. (2006), "Power-electronic systems for the grid integration of renewable energy sources: A survey," IEEE Trans. Ind. Electron., vol. 53, no. 4, pp. 1002–1016.

Suh, Sinha.G, Manjrekar.M.D & Lipo.T.A. (1998), "Multilevel power conversion—An overview of topologies and modulation strategies," in Proc. OPTIM, May 14–15, vol. 2, pp. AD-11–AD-24.

Wu. B. (2005) "High-power converters and AC drives," in Proc. IEEE PESC, Recife, Brazil, Jun. 12–18.

Bendre, G. Venkataramanan, Rosene.D & Srinivasan.V. (2006), "Modeling and design of a neutral-point voltage regulator for a three-level diode clamped inverter using multiple-carrier modulation," IEEE Trans. Ind. Electron., vol. 53, no. 3, pp. 718–726.

Yacoubi.L, Haddad.K, Dessaint. L. A & Fnaiech.F. (2006) , "Linear and nonlinear control techniques for a three-phase three-level NPC boost rectifier," IEEE Trans. Ind. Electron., vol. 53, no. 6, pp. 1908–1918.

Vargas.R, Cortes.P, Ammann.U, Rodriguez.J & Pontt J. (2007), "Predictive control of a three-phase neutral-point-clamped inverter," IEEE Trans. Ind. Electron., vol. 47, no. 2, pp. 2697–2705.

Kim.I. D, Nho.E.C, Kim.H. G & Ko.J.S. (2004), "A generalized undeland snubber for flying capacitor multilevel inverter and converter," IEEE Trans. Ind. Electron., vol. 51, no. 6, pp. 1290–1296.

Du.Z,Tolbert.L.M,Chiasson.J.N, Ozpineci.B, Hui.L & Huang.A.Q.(2006), "Hybrid cascaded H-bridges multilevel motor drive control for electric vehicles," in Proc. IEEE Power Electron.

Hanna.R.A & Prabhu.S.(1997), "Medium-voltage adjustable-speed drives users and manufacturers' experiences," IEEE Trans. Ind. Appl., vol. 33, no. 6, pp. 1407–1415.

Rech.C&Pinheiro.J.R.(2007),"Hybrid multilevel converters: Unified analysis and design considerations," IEEE Trans. Ind. Electron., vol.54, no. 2, pp. 1092–1104.

Robicon Perfect Harmony Medium Voltage AC Drives. [Online]. Available: <http://www.siemens.com>

Cengelci.E, Sulistijo.S.U, Woo.B.O, Enjeti.P, Teoderescu.R, & Blaabjerg.F(1999), "A new medium-voltage PWM inverter topology for adjustable-speed drives," IEEE Trans. Ind. Appl., vol. 35, no. 3, pp. 628–637.

Wen.J & Smedley.K, "New converters for high power applications." U.S and International patents pending.

Wen.J & Smedley.K(2008), "A new multilevel inverter–Hexagram inverter for medium- voltage adjustable speed drive systems. Part II. Three-phase motor drive," Proc. IEEE PESC, Orlando, FL, Jun. 15–19, pp. 1571–1577.

Wen.J & Smedley.K (2007), "A new multilevel inverter–Hexagram inverter for medium - voltage adjustable speed drives systems. Part I. Six-phase motor drive," in Proc. POWERENG, Setubal, Portugal.

Wen.J & Smedley.K(2008),"Hexagram Inverter for Medium-Voltage Six-Phase Variable drives" IEEE Trans. Ind. Electron., vol. 55, no. 6, pp. 2473–2481.

Wen.J & Smedley.K(2008),"Hexagram rectifier-Active front end for medium voltage adjustable speed drive systems," in Proc. IEEE Transmiss.Distrib. Conf. Expo., Chicago, IL.

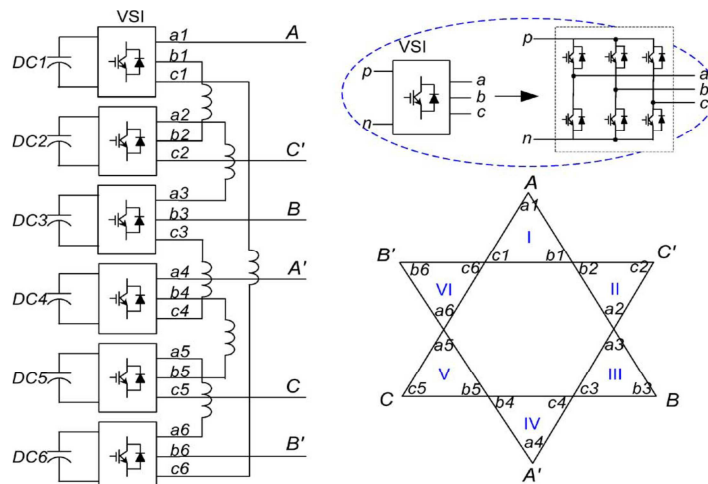


Figure 1. Hexagram inverter.

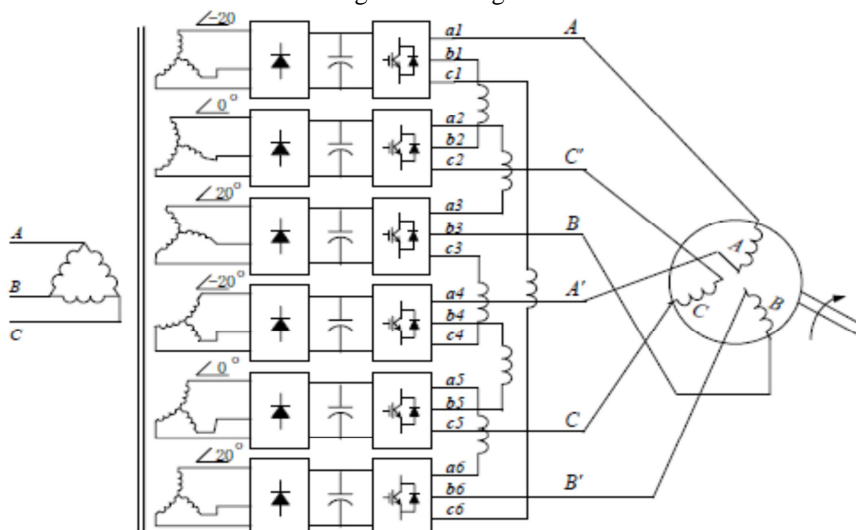


Figure 2. Hexagram inverter for a three phase induction motor drive.

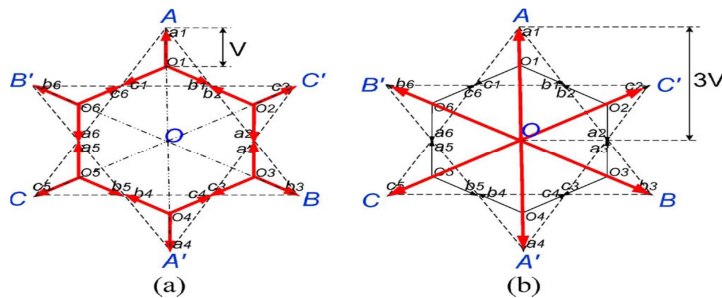


Figure 3. Voltage phasor diagram of the Hexagram inverter. (a) Phase Voltages of VSI modules. (b) Output Voltages of the Hexagram inverter.

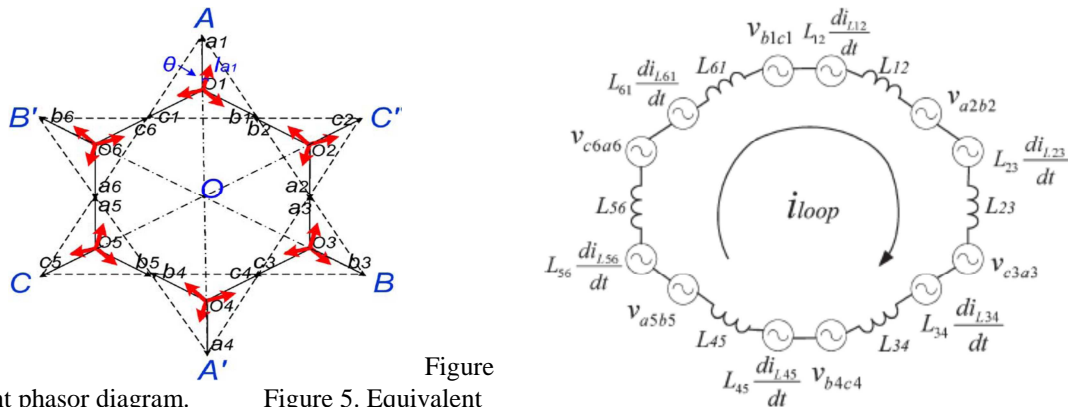


Figure 4. Current phasor diagram. Figure 5. Equivalent circuit of the circulating current.

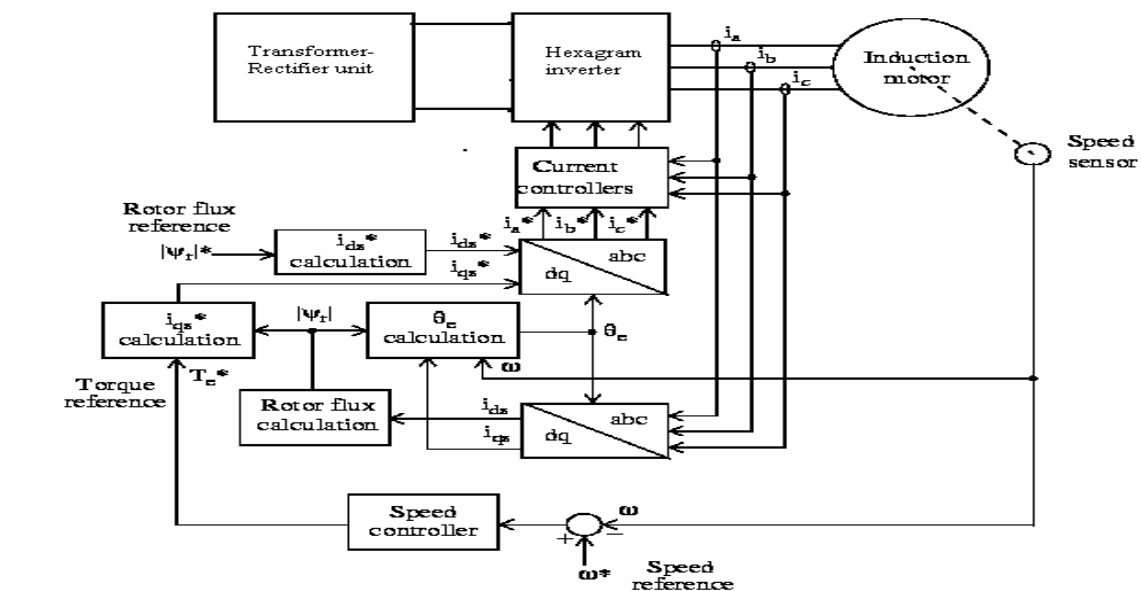


Figure 6. Closed loop control of hexagram inverter drive.



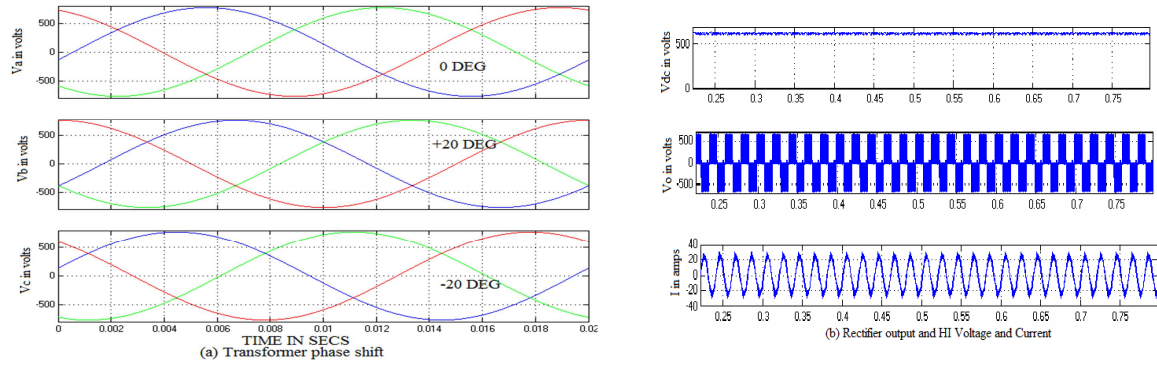


Figure 7. Simulation results of Hexagram inverter.

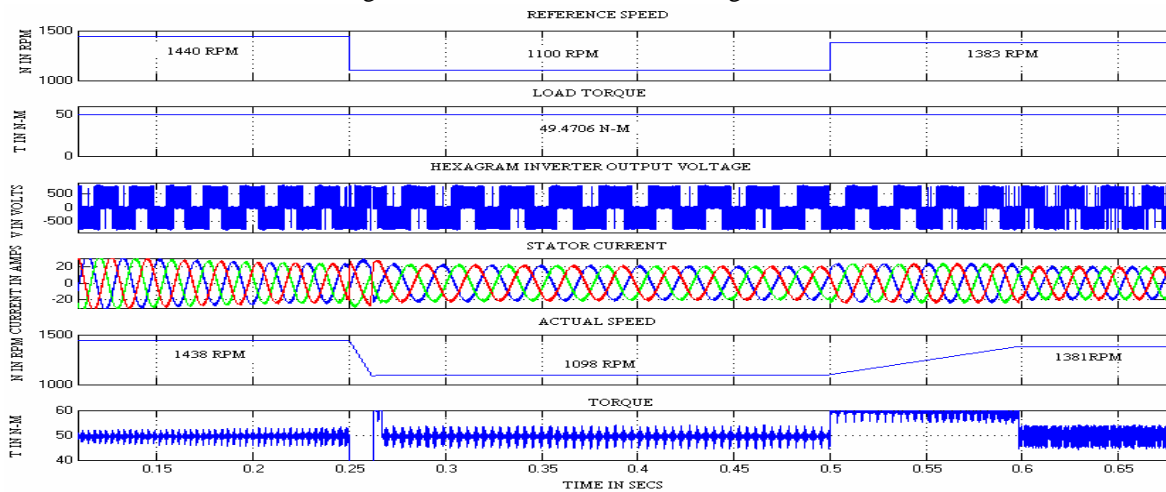


Figure 8. Dynamic response of Hexagram inverter drive for varying speed.

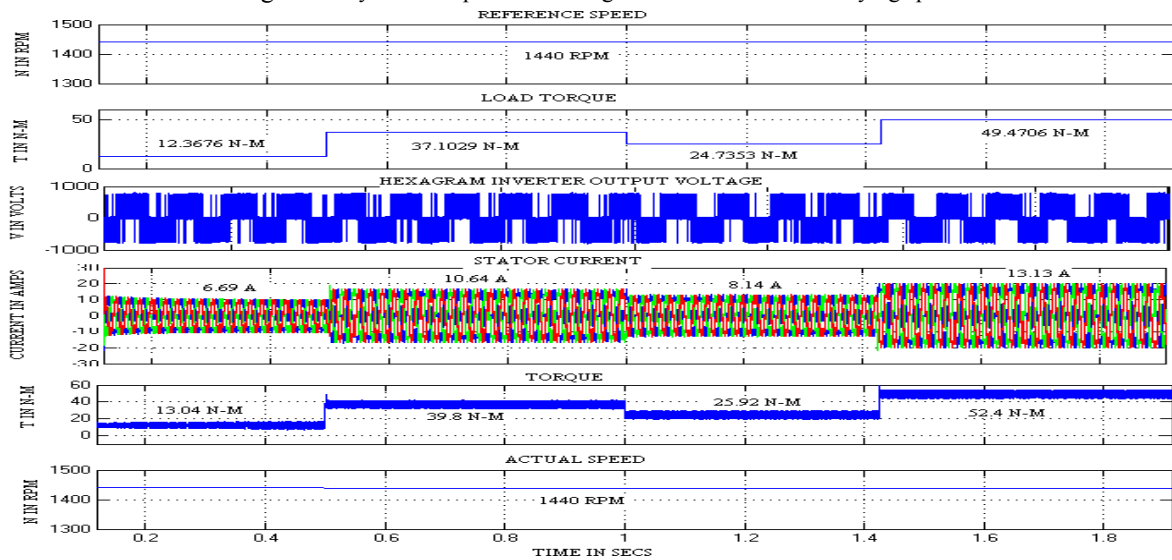


Figure 9. Dynamic response of Hexagram inverter drive for varying torque.

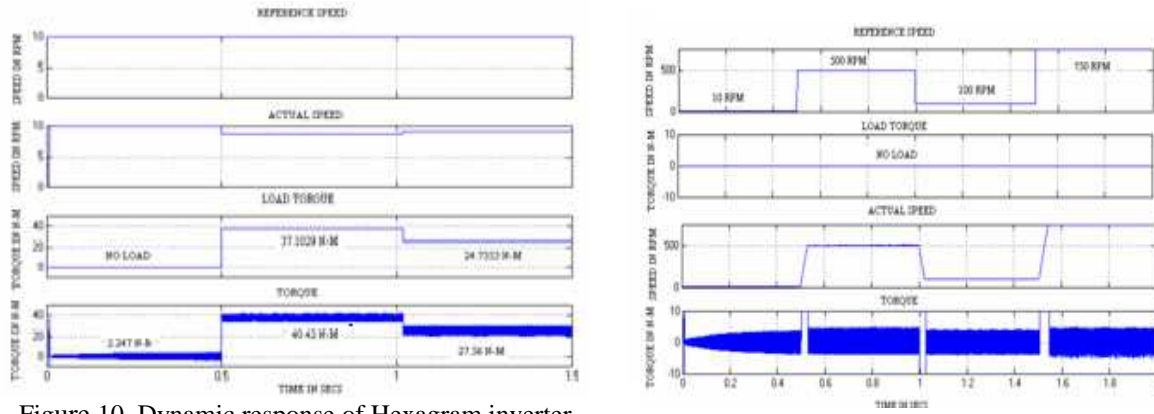


Figure 10. Dynamic response of Hexagram inverter drive for low speed /less torque.

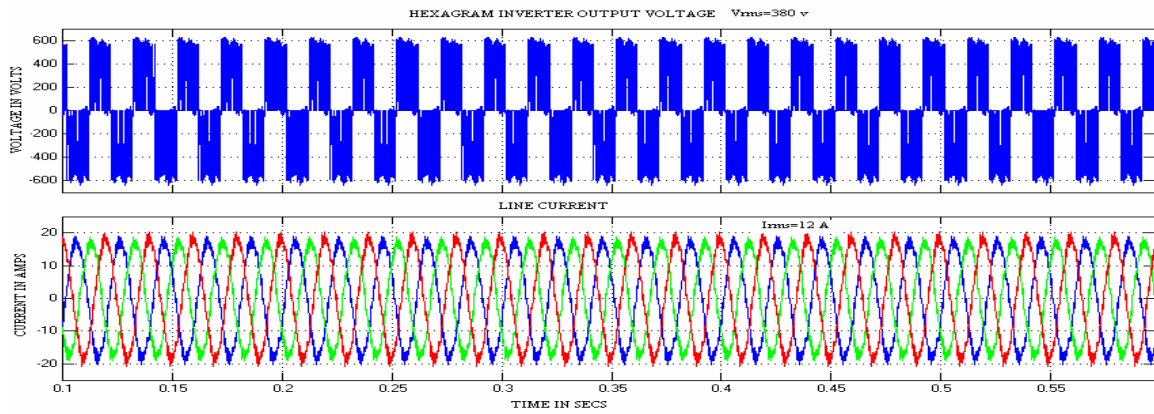


Figure 11. Fault tolerant feature of the Hexagram Inverter.

Table 1. Comparison of Hexagram inverter with cascaded H-bridge inverter.

Comparison condition	Multilevel Inverter	Hexagram Inverter
No. of secondary windings	12	6
No. of Diode bridge rectifiers	12	6
No. of Power switches	48	36
No. of Inductors	0	6
No. of capacitors	12	6

Table 2.  
Voltage

variation of the Hexagram inverter for different Modulation indices.

Different load conditions	MI-0.6		MI-0.8		MI-1	
	$V_L$	$N_r$	$V_L$	$N_r$	$V_L$	$N_r$
No load	365.7	1498	419	1499	640	1376
25% load	358.3	1454	413.1	1471	443.9	1523
50% load	357.5	1399	412.5	1447	517.8	1442
75% load	357.5	1330	412	1418	551.1	1360
100% load	357.1	1229	412.6	1383	443.9	1523

This academic article was published by The International Institute for Science, Technology and Education (IISTE). The IISTE is a pioneer in the Open Access Publishing service based in the U.S. and Europe. The aim of the institute is Accelerating Global Knowledge Sharing.

More information about the publisher can be found in the IISTE's homepage:

<http://www.iiste.org>

The IISTE is currently hosting more than 30 peer-reviewed academic journals and collaborating with academic institutions around the world. **Prospective authors of IISTE journals can find the submission instruction on the following page:**

<http://www.iiste.org/Journals/>

The IISTE editorial team promises to review and publish all the qualified submissions in a fast manner. All the journals articles are available online to the readers all over the world without financial, legal, or technical barriers other than those inseparable from gaining access to the internet itself. Printed version of the journals is also available upon request of readers and authors.

### **IISTE Knowledge Sharing Partners**

EBSCO, Index Copernicus, Ulrich's Periodicals Directory, JournalTOCS, PKP Open Archives Harvester, Bielefeld Academic Search Engine, Elektronische Zeitschriftenbibliothek EZB, Open J-Gate, OCLC WorldCat, Universe Digital Library, NewJour, Google Scholar

